Gating of a mechanosensitive channel due to cellular flows

On Shun Pak[a], Y.-N. Young[b], Gary R. Marple[c], Shravan Veerapaneni[c], and Howard A. Stone[d,1]

[a]Department of Mechanical Engineering, Santa Clara University, Santa Clara, CA 95053; [b]Department of Mathematical Sciences, New Jersey Institute of Technology, Newark, NJ 07102; [c]Department of Mathematics, University of Michigan, Ann Arbor, MI 48109; and [d]Department of Mechanical and Aerospace Engineering, Princeton University, Princeton, NJ 08544

Contributed by Howard A. Stone, June 27, 2015 (sent for review February 6, 2015)

A multiscale continuum model is constructed for a mechanosensitive (MS) channel gated by tension in a lipid bilayer membrane under stresses due to fluid flows. We illustrate that for typical physiological conditions vesicle hydrodynamics driven by a fluid flow may render the membrane tension sufficiently large to gate a MS channel open. In particular, we focus on the dynamic opening/closing of a MS channel in a vesicle membrane under a planar shear flow and a pressure-driven flow across a constriction channel. Our modeling and numerical simulation results quantify the critical flow strength or flow channel geometry for intracellular transport through a MS channel. In particular, we determine the percentage of MS channels that are open or closed as a function of the relevant measure of flow strength. The modeling and simulation results imply that for fluid flows that are physiologically relevant and realizable in microfluidic configurations stress-induced intracellular transport across the lipid membrane can be achieved by the gating of reconstituted MS channels, which can be useful for designing drug delivery in medical therapy and understanding complicated mechanotransduction.

mechanosensitive channels | vesicles | viscous flow | drug delivery | nanoparticle delivery

Mechanosensitive (MS) channels are essential to mechanosensation and mechanotransduction in a wide range of cells (1–3). Due to the great diversity of MS channels, the general gating mechanism is found to depend on combinations of the detailed molecular structures (4–7), the gating-associated conformational changes (8–10), and coupling with the lipid bilayer membrane (11–14). It remains a challenge to elucidate general mechanisms underpinning the gating of MS channels. In this spirit it is useful to have "simple" models to understand the complex response of MS channels and their associated biological functions (15).

Stretch-activated (SA) channels are a class of (relatively) simpler MS channels that are stretched open mainly by membrane tension (e.g., due to osmotic shock, stress from fluid flow, or other mechanical sources of tension) for nonselective intracellular transport of ions and macromolecules (16–19). Their gating mechanisms have been investigated by experiments (18), continuum modeling (20, 21), and molecular dynamics (MD) simulations (22). By exerting an unphysiologically large load onto a membrane patch with a single SA channel in the center, MD simulations show that a SA channel (several nanometers in size) responds to membrane tension within a few nanoseconds (22). Due to computational limitations, MD simulations are restricted to a small lipid patch and a short timescale (approximately microseconds). On the other hand, continuum modeling has been adopted widely in recent studies where the transduction of membrane tension to SA channels is found to depend on the molecular details of lipid binding in the channels (13). For example, the channel gating was shown to depend on the protein surface charge and hydrophobicity (23).

Novel technological advancements in microfluidics have made it possible to construct artificial vesicles (of tens of micrometers in size) reconstituted with MS channels (24). Furthermore, recent experiments on dynamic conductance of MS channels in vesicles show that the oscillatory fluid stress is sufficient to cause large tension in the membrane and the gating of MS channels (25). Such idealized model systems for gating of MS channels in cells are suitable for elucidating the detailed gating mechanism coupled with the membrane dynamics, which is intrinsically multiscale both in space and in time. Coarse-grained MD simulations of such systems would take too long, given the current computational power, and thus are not practical.

Motivated by the recent success of continuum modeling of MS channels (13, 20, 23), in this paper we propose a multiscale continuum model to study the gating of a single MS channel by tension in a membrane exposed to fluid stress. In particular, as highlighted in Fig. 1, we aim to address how a nanosize MS channel in a model bilayer can be activated by flow-generated stresses by focusing on two typical physiological flows involving vesicles: a planar shear flow and flow through a narrowing constriction. For example, recently a microfluidic platform has been reported for intracellular delivery of macromolecules into a highly deformed cell as it passes through a narrow constriction (26). Here we illustrate that a similar microfluidic constriction flow can gate a MS channel open for intracellular delivery. Our modeling work focuses on a SA channel, and for simplicity we refer to it generally as a MS channel for the rest of the paper.

In our model the lipid bilayer membrane is assumed to be locally inextensible because a fluid-phase lipid bilayer membrane can be stretched only no more than 5% before rupture. When exposed to shear stress a vesicle deforms and membrane tension develops to enforce local inextensibility (constant surface area). Therefore, the membrane tension, which depends on external flow, is expected to be spatially varying, and a balance between

Significance

Mechanosensitive (MS) channels are membrane proteins that can be gated by membrane tension, and they play major roles in mechanosensation and mechanotransduction in cells. As a step in understanding the dynamics of a MS channel in membranes exposed to fluid flows, a multiscale continuum model is constructed to address how a MS channel in a vesicle membrane can be gated by flow-generated stresses in two physiological flows: planar shear flow and pressure-driven flow across a constriction channel. We demonstrate the opening/closing of a MS channel as a function of the flow strength and physical parameters. Our numerical results also suggest the possibility of utilizing fluid flows to deliver macromolecules (e.g., drugs) by gating MS channels reconstituted in liposomes in microfluidic platforms.

Author contributions: O.S.P., Y.-N.Y., and H.A.S. designed research; O.S.P., Y.-N.Y., G.R.M., S.V., and H.A.S. performed research; O.S.P., Y.-N.Y., S.V., and H.A.S. analyzed data; and O.S.P., Y.-N.Y., S.V., and H.A.S. wrote the paper.

The authors declare no conflict of interest.

[1]To whom correspondence should be addressed. Email: hastone@princeton.edu.

This article contains supporting information online at www.pnas.org/lookup/suppl/doi:10.1073/pnas.1512152112/-/DCSupplemental.

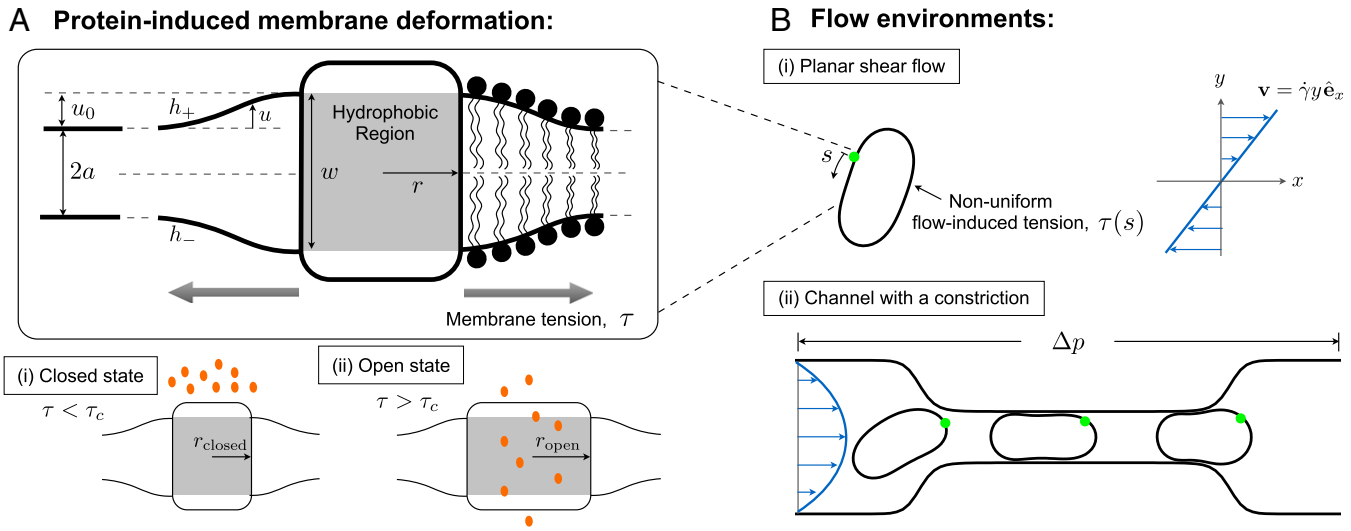

Fig. 1. Multiscale characterization of a stretch-activated, membrane-bound channel in a flow. (*A*) Schematic representation of the protein-induced membrane deformation. Ions are either unable or allowed to cross the membrane, depending, respectively, on whether the channel is in the closed (*i*) or open (*ii*) state. (*B*, *i*) A 2D vesicle, with s as the arc length along the membrane, in a linear shear flow, $\mathbf{v} = \dot{\gamma} y \hat{\mathbf{e}}_x$, where $\dot{\gamma}$ is the shear rate and y is the coordinate in the direction of the shear gradient. (*B*, *ii*) A vesicle entering and translating through a constriction due to a pressure-driven flow. The green circle on the membrane in *B* indicates a MS channel.

bending force, membrane tension, and hydrodynamic force (27, 28) leads to different vesicle dynamics.

In a planar shear flow, a vesicle membrane exhibits tank-treading, tumbling, breathing, and ventilating modes of motion depending on the shear rate, viscosity mismatch (between inner and outer fluids), and vesicle excess area (or reduced volume). Numerical results show that as a consequence of fluid motion the membrane tension varies both spatially and temporally as it deforms due to the external stress. Because the MS channel size is comparable to the membrane thickness and they are both smaller than the size of the vesicle, the interaction between a single channel and the lipid bilayer membrane dynamics is a one-way coupling within the continuum modeling: The membrane hydrodynamics are not affected by the channel state, which depends on the membrane tension at the channel location. In addition, the diffusive transport of a transmembrane protein is negligible compared with the velocity on the vesicle under typical flow conditions in the microfluidic experiments. Therefore, we neglect the diffusive transport of the MS channel in the vesicle membrane (see *SI Appendix* for an order of magnitude estimate). Instead we focus on the channel state (open or closed) as it moves along the vesicle (at the membrane velocity), experiencing the local membrane tension that results from vesicle hydrodynamics in two flow configurations: a planar shear flow and a pressure-driven flow across a narrow constriction. Results from these analyses and numerical simulations will shed light on hydrodynamically induced molecular transport across lipid bilayer membranes (26).

Formulation

The complex interactions between lipids and transmembrane proteins depend on details of the proteins and cell types. In this work we consider the effects of fluid flows on the simplest model mechanosensitive system, which is a framework developed by Wiggins and Phillips (20) for studying mechanotransduction where the mechanical interaction between a MS channel and the bilayer membrane arises from the competition between the free energy due to membrane tension and deformation energy induced by hydrophobic mismatch. Although the modeling results in ref. 20 were compared only with experimental data of bacterial MS channels, we expect the underlying physics to be a general mechanical feature of MS channels in different mechanosensitive systems. The previous model assumes a planar lipid bilayer membrane with a constant tension and has also been extended to the interaction between two MS channels (29). For a constant membrane tension the mechanical gating of a MS channel is consistent with experimental observations (20). In many situations, however, the tension of a cytoplasmic membrane can vary in position and time as a cell encounters changes in hydrodynamic stress, which occurs, for example, as cells enter or exit narrowing constrictions in physiological flow networks (30). In experiments it has not been possible to measure the tension along the cell membrane as the cell deforms when it flows through such geometries. On the other hand, theoretical analyses (27) and numerical simulations (31–33) of continuum models show that the membrane tension varies significantly as a cell or vesicle undergoes large deformation under flow. Therefore, in our multiscale modeling we allow the tension τ (force/length) to vary with arc length s along a 2D membrane of length ℓ (Fig. 1*B*).

We denote the positions of the lipid bilayer membrane leaflets as h_+ and h_- (Fig. 1*A*). Without the MS channel the bilayer membrane is assumed to have a uniform thickness $2a$ at equilibrium. In the presence of a MS channel, the mismatch between the hydrophobic region of the protein w and the bilayer equilibrium thickness $2a$ (see Fig. 1 for notations) induces a thickness variation u along the membrane, denoted as $u = (h_+ - h_- - 2a)/2$. Following the development of Wiggins and Phillips (20) and Haselwandter and Phillips (29, 34), the free energy E of a cylindrical MS channel (of radius r, Fig. 1*A*) embedded in a lipid bilayer membrane can be formulated in the continuum framework as

$$E = G_h 2\pi r - \tau_0 \pi r^2, \qquad [1]$$

where G_h corresponds to the free energy per unit length associated with the membrane thickness variation due to the hydrophobic mismatch, and $\tau_0 \pi r^2$ is the free energy of the loading associated with the local membrane tension $\tau_0 = \tau(s = 0, t)$ at the channel. Following ref. 20 we assume that (*i*) the surface integral of the elastic energy due to the membrane thickness variation u may be approximated as the product of the energy per unit length G_h with the circumference of the channel $2\pi r$,

Table 1. Summary of physical parameters of the bilayer membrane and the MS channel and their values used in this study

Dimensional parameters	Symbols	Values
Bending modulus	K_b	20 k_BT
Expansion modulus	K_t	30 k_BT/nm^2
Hydrophobic mismatch	$2u_0$	0.2 nm
Undeformed bilayer thickness	$2a$	4 nm
Channel radius at the closed state	r_{closed}	3 nm
Channel radius at the open state	r_{open}	5 nm
Equivalent vesicle radius	R_0	0.1 μm

(*ii*) the contributions of spontaneous curvature and midplane deformation to the free energy may be neglected, and (*iii*) due to steric constraints the channel radius can only vary within a range $r_{closed} \le r \le r_{open}$. The channel is in the closed state when the minimum total free energy occurs at $r = r_{closed}$; similarly, the channel attains an open state when the minimum total free energy occurs at $r = r_{open}$.

For the 2D case considered here, the elastic energy per unit length G_h due to membrane thickness variation u is given by

$$G_h = \frac{1}{2}\int_0^\ell \left[K_b\left(\nabla^2 u\right)^2 + K_t\left(\frac{u}{a}\right)^2 + \tau\left(\frac{2u}{a} + (\nabla u)^2\right)\right] ds, \qquad [2]$$

where K_b is the bending rigidity of the lipid bilayer, K_t is the stiffness associated with membrane thickness deformation u, and τ is the distribution of tension. The variation of Eq. **2** gives the governing equation for u:

$$\nabla^4 u + \frac{K_t}{K_b a^2}u - \frac{\nabla\cdot(\tau\nabla u)}{K_b} + \frac{\tau}{K_b a} = 0. \qquad [3]$$

At the MS channel ($s = 0$ and $s = \ell$), the thickness variation u is constrained by the hydrophobic mismatch $u|_{s=0} = u|_{s=\ell} = u_0$, and we assume the bilayer membrane meets the protein at zero slope (35), $\partial u/\partial s|_{s=0} = \partial u/\partial s|_{s=\ell} = 0$. The MS channel is coupled to the membrane hydrodynamics via the membrane tension τ, which is determined from the force balance on an elastic inextensible 2D vesicle in a Stokes flow as described next.

Vesicle Dynamics. The dynamics of an elastic inextensible 2D vesicle suspended in a flow are governed by a balance between the nonlocal hydrodynamic forces and the elastic forces due to bending and tension along the membrane. We use the boundary integral formulation (32, 36) to solve for the vesicle shape evolution and dynamics. Our goal is to extract the membrane tension $\tau(s)$ for given flow conditions via numerical simulations and use $\tau(s)$ to determine the thickness variation $u(s)$ by solving Eq. **3**. Then we determine E and G_h using, respectively, Eqs. **1** and **2**. A summary of the equations and a numerical algorithm for solving this hierarchical continuum model are provided in *SI Appendix*.

Parameter Values and Scaling. The values of the model parameters depend on specific proteins and membrane properties. We illustrate our model using values that are of the same order of magnitude as typical measured values (20, 37) (Table 1). The thickness deformation u is scaled by the nonzero hydrophobic mismatch u_0 and the arc length along the 2D enclosed membrane s is scaled by $R_0 = \ell/2\pi$, which is the radius of a circle having the same perimeter as the vesicle, i.e., $s/R_0 \in [0, 2\pi]$. The membrane tension and free energy of a MS channel are scaled, respectively, by K_b/R_0^2 and $K_t u_0^2$. Refer to *SI Appendix* for the dimensionless equations and boundary conditions. Below we highlight the energy E (Eq. **1**), which dictates the state of the MS channel.

Results

We investigate the effects of different mechanical environments on the gating of a MS channel, which in general render the membrane tension nonuniform. Before presenting the results for different cellular-type flows, we first illustrate the features of the model by prescribing a uniform tension along the vesicle, which extends the results of Wiggins and Phillips (20) to the case of an enclosed membrane. In particular, we derive the critical tension for opening a MS channel.

Uniform Membrane Tension. The analysis is simplified when a uniform membrane tension $\bar{\tau}$ is prescribed in Eq. **3**. This case allows an analytical solution for the thickness variation $u(s)$ and hence the total free energy of a MS channel (*SI Appendix*). Given the parameter values in Table 1 and a prescribed $\bar{\tau}$, the free energy E is only a function of the channel radius r (Eq. **1**), which is shown in dimensionless form in Fig. 2 for different values of the uniform membrane tension. Due to steric constraints, the channel radii outside the range $[r_{closed}, r_{open}] = [3,5]$nm are not accessible (Fig. 2, yellow shading). For $\bar{\tau}/(K_b/R_0^2) = 14$ (Fig. 2, blue line), the minimum energy is attained at $r = r_{closed}$; i.e., the MS channel remains closed.

The channel is expected to open when the membrane tension is sufficiently large. This critical tension $\bar{\tau}_c$ can be calculated by the condition that the energies of the open and closed states are equal, which results in a transcendental equation for $\bar{\tau}_c$,

$$\frac{\bar{\tau}_c}{G_h(\bar{\tau}_c)} = \frac{2}{r_{open} + r_{closed}}, \qquad [4]$$

where $G_h(\bar{\tau}_c)$ is given by the integral in Eq. **2**. Should G_h be independent of the membrane tension, Eq. **4** is no longer transcendental and reduces to that given in refs. 20 and 37 for the planar case. With the parameter values in Table 1, we solve Eq. **4** numerically for the critical tension, $\bar{\tau}_c/(K_b/R_0^2) = 16.3$. The corresponding energy landscape at this critical membrane tension is shown in Fig. 2 (red line). Beyond this critical tension [e.g., $\bar{\tau}/(K_b/R_0^2) = 18$], the lowest energy is attained at $r = r_{open}$ (green line in Fig. 2); i.e., the MS channel is in the open state. Thus, in the spirit of refs. 20 and 37 we have demonstrated an algorithm

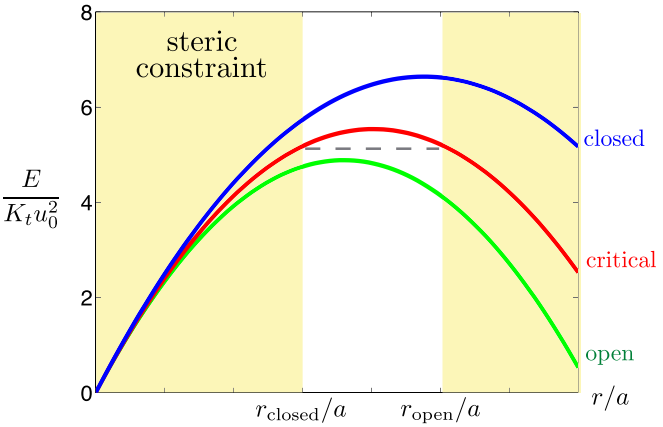

Fig. 2. Energy landscape of a MS channel as a function of (dimensionless) channel radius r for different values of the uniform membrane tension, $\bar{\tau}/(K_b/R_0^2) = 14$ (blue line), 16.3 (red line), and 18 (green line), which correspond, respectively, to closed, critical, and open states. The yellow-shaded regions ($r < r_{closed} = 3$ nm and $r > r_{open} = 5$ nm) are not accessible due to steric constraints.

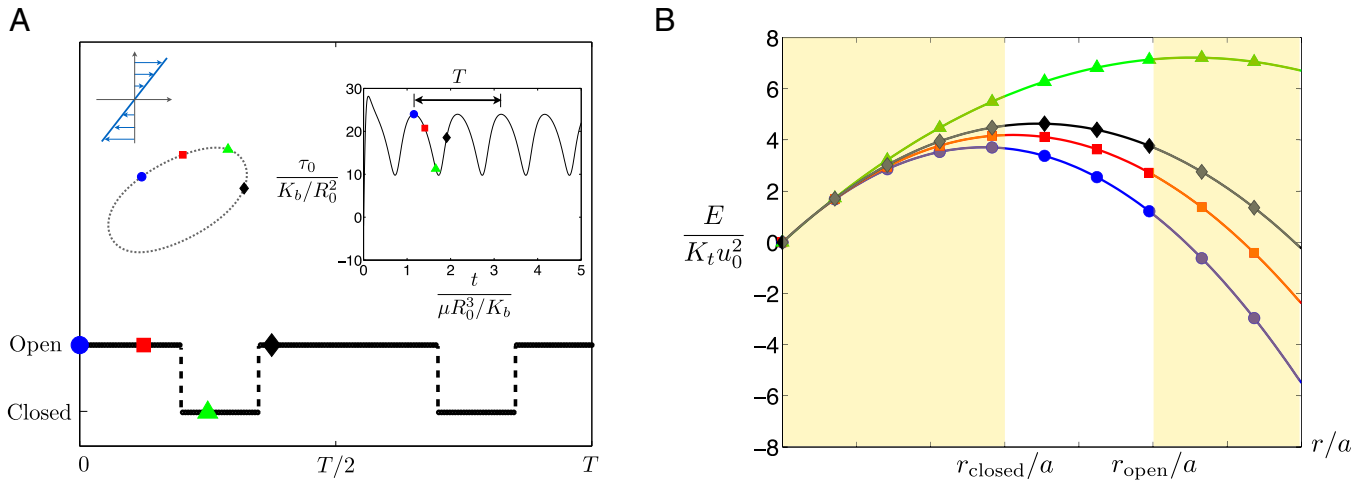

Fig. 3. Gating of a mechanosensitive channel on a vesicle subject to a shear flow at Ca = 8. (*A*) The state (open/closed) of the MS channel as a function of time in a period *T*, where *Insets* show the steady-state shape of the vesicle (*Left*) and the local membrane tension at the MS channel location as a function of time (*Right*). (*B*) Energy landscape of the MS channel as a function of channel radius *r* at different times (or locations on the membrane). The symbols blue circle, red square, green triangle, and black diamond represent the MS channel at time instants separated by intervals of *T*/8.

for membrane tension regulating the opening and closing of a MS channel.

Planar Linear Shear Flow. Shear flows have been proposed as a means for controlling the membrane permeability (38). Here we use our multiscale model to address whether a steady shear flow can induce gating of MS channels in a vesicle. A vesicle in a planar shear flow deforms and the membrane tension varies spatially as a result of inextensibility. For simplicity we assume that the fluid viscosities inside and outside the vesicle are the same, and hence the vesicle takes a steady equilibrium shape in shear flow with a tank-treading motion along the membrane (rolling motion of the membrane about its interior while maintaining a constant shape) (27). The shear flow is characterized by a dimensionless shear rate (or a capillary number) given by $\text{Ca} = \dot{\gamma}\mu R_0^3/K_b$. For a vesicle with $R_0 \approx 0.1 - 10$ μm, physiological shear rates $\dot{\gamma} \approx 1 - 10^3$ s^{-1}, and $\mu \approx 1$ m Pa s, then $\text{Ca} \approx 0.25 - 10$. For a given Ca, the vesicle attains a steady-state shape with an inclination relative to the horizontal axis (see Fig. 3*A*, *Left Inset* for the shape at Ca = 8).

We define a period T as the time it takes for a Lagrangian marker on the tank-treading membrane to complete one cycle and return to its original position. Ignoring in-plane protein diffusion relative to the effects of the tank-treading speed (*SI Appendix*), we assume that a MS channel moves with the local fluid velocity along the membrane. In Fig. 3*A*, *Left Inset* we consider a MS channel in the location represented by the blue circle, where the local membrane tension is maximum (Fig. 3*A*, *Right Inset*), and its subsequent locations along the membrane, over a half period, at fixed time intervals ($T/8$) by the red square, a green triangle, and a black diamond; the dynamics for the other half period are similar. The channel protein moves along the membrane and hence samples the local tension τ_0 at different times (Fig. 3*A*, *Right Inset*). The energy landscape of the MS channel is therefore a periodic function of time or location along the membrane (Fig. 3*B*).

As a result of the variations in tension, the state of a MS channel depends on its location on the membrane. Our model reveals the time history of the state of a MS channel as it travels along the membrane (Fig. 3*A*). At the location with maximum local membrane tension (blue circle in Fig. 3*A*), a MS channel is in the open state (corresponding energy landscape in Fig. 3*B*, blue line). The channel remains open until the protein approaches the elongated end of the vesicle (between the green triangle and the black diamond in Fig. 3), where the free energy is minimum at $r = r_{\text{closed}}$ (Fig. 3*B*, green line). As shown in the time history of local tension sampled by a moving MS channel (Fig. 3*A*, *Right Inset*), the vesicle has low membrane tension around the elongated end, which is a main reason for the closed state being the more energetically favorable state in these regions. When the protein departs from the elongated end, it resumes the open state (black diamond in Fig. 3*A* and black line in Fig. 3*B*). The magnitude of the membrane tension here is at least an order of magnitude smaller than the lysis tension, ensuring membrane integrity.

For a low shear rate (e.g., Ca = 3), the lowest energy states always occur at the closed state (*SI Appendix*, Fig. S1 *A* and *B*), regardless of the location of a MS channel on the membrane. A MS channel therefore remains closed as the protein travels along the membrane. When Ca is sufficiently large, a MS channel can remain always open throughout its journey along the entire membrane, which is the case, for instance, at Ca = 13 (*SI Appendix*, Fig. S1 *C* and *D*).

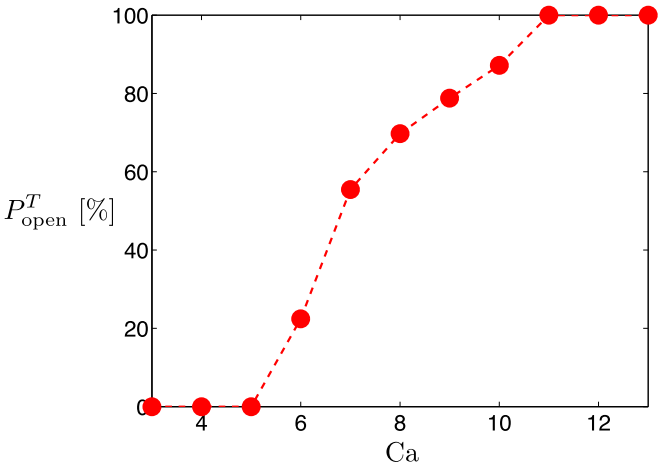

Fig. 4. Percentage of time a MS channel spends in the open state over one period, P^T_{open}, as a function of the dimensionless shear rate, Ca. The dotted lines represent linear interpolations between numerical data.

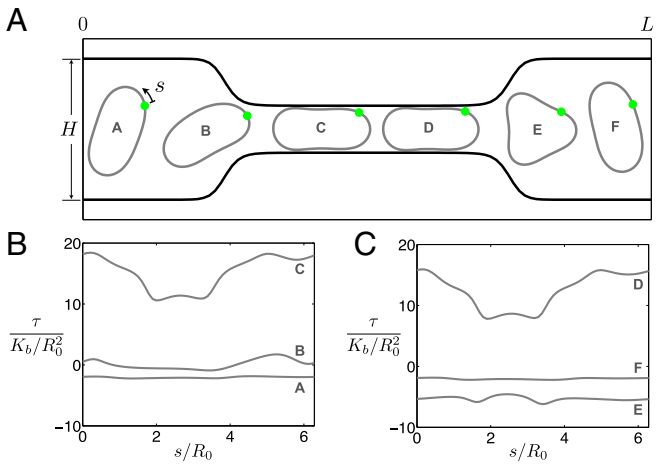

Fig. 5. Dynamics of a 2D vesicle through a channel with a constriction. (*A*) Deformation of a vesicle at different locations inside the channel. The green circle represents the location of a MS channel ($s=0$). (*B* and *C*) Membrane tension profiles along the vesicle at the corresponding locations inside the channel shown in *A*. Geometric parameters of the channel and constriction (scaled by R_0): $L/R_0=15.6$, $H/R_0=3.86$. The length and width of the constriction are, respectively, $L/2$ and $H/3$. The nondimensionalized pressure difference is $\Delta p R_0^3 H/(K_b L)=8.17$.

For a single MS channel traveling along the vesicle in one period, the percentage of time a MS channel spends in the open state in one period, P^T_{open}, can be calculated as a function of Ca (Fig. 4). With the parameter values in Table 1, a MS channel remains always closed when $\text{Ca}\lesssim 5$ and becomes fully open when $\text{Ca}\gtrsim 11$ (Fig. 4). The results demonstrate quantitatively how varying the shear rate acts as a mechanism to switch on and off a MS channel and control the membrane permeability.

Vesicle in a Channel Flow with a Constriction. Finally, we consider how sudden changes in geometry affect the gating of MS channels. To do so we consider a standard configuration where a vesicle with a MS channel is suspended in a pressure-driven channel flow with a constriction (Fig. 5*A*). Such geometries are common physiological and experimental environments; for instance, RBCs often go through constrictions 30–80% smaller than their diameters, and microfluidic flow channels with similar geometry have been used for intracellular delivery of macromolecules into multiple cell types (26). Unlike the case of planar shear flows, the vesicle does not admit a steady-state shape but continuously deforms as it flows along the channel, especially when entering and leaving the constriction (see Fig. 5*A* for the vesicle shape at different locations in the channel). In this case, a control parameter is the pressure drop Δp across the constriction.

The vesicle therefore has different tension profiles along the membrane, depending on its location in the channel. For the vesicle locations in the channel displayed in Fig. 5*A*, the corresponding tensions $\tau(s)$ are shown in Fig. 5 *B* and *C*. We observe that the membrane tension generally increases as the vesicle enters the constriction and decreases when it leaves the constriction. It is therefore expected that the constriction can serve as an external mechanism to control the ion channel gating on a vesicle. Due to the increased membrane tension, an ion channel may open during its time inside the constriction.

For the case of a vesicle tank treading in shear flows discussed earlier, a single MS channel travels along the membrane and experiences local membrane tension in one period. In contrast, for the case of a channel flow with a constriction, a MS channel does not travel around the entire membrane when the vesicle flows through the channel (green circle in Fig. 5*A*). The initial location of a MS channel is therefore important because the channel protein samples only a portion of the membrane tension profile. To quantify the MS channel dynamics using our multiscale model, we place a MS channel at 1 of 64 different locations on the membrane, represented by symbols along the vesicle in Fig. 6*A*. We then determine whether the MS channel would be in the closed or the open state (represented by blue asterisks and red open circles, respectively) at these locations on the vesicle as it passes through the constriction. When the vesicle enters the constriction, the MS protein in the front half of the membrane begins to open (Fig. 6*A*). The percentage of open MS channels, P^N_{open}, is calculated as a function of the vesicle position as it travels through the channel (Fig. 6*B*). For the conditions of the simulations, a maximum of ~53% of MS channels on the membrane would be open when the vesicle is about midway in the constriction. Because a MS channel does not travel around the vesicle, a MS channel initially located in the low membrane tension region may stay closed as the vesicle enters and leaves the constriction.

Discussion

We have presented a multiscale continuum formulation to couple the gating of a MS channel with the dynamics of a lipid bilayer membrane under flow. When applied to a tank-treading vesicle in a planar shear flow, our model indicates that embedded

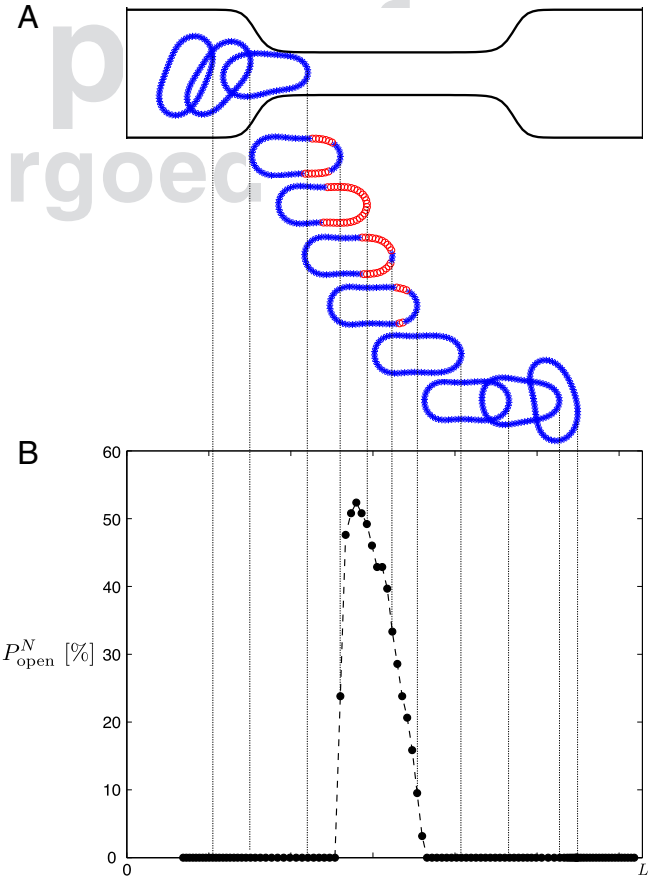

Fig. 6. (*A*) Visualization of the state of a MS channel as the vesicle flows inside a channel. Symbols (blue asterisks and red open circles) on the membrane represent 64 different locations of the MS channel on the membrane. The closed state is represented by blue asterisks and the open state is represented by red open circles. (*B*) Percentage of the number of locations where the MS channel is at the open state as the vesicle passes through different locations along the channel.

MS channels can be open in some locations on the membrane for sufficiently large shear rates. When applied to a vesicle going through a microfluidic channel with a constriction, we find that MS channels are open mostly right after the entry to the constriction where the largest deformations are observed. As the vesicle adjusts inside the constriction, the tension is reduced in magnitude and the MS channels close.

We emphasize that the simple model system considered here pertains to mechanosensitive systems where the bilayer-inclusion interaction is described by the competition between membrane tension and deformation induced by hydrophobic mismatch. Different mechanisms affecting the competition are expected for different cell types. In particular, our framework is relevant to bacterial cells (20), even though the main principle is expected to be applicable for other cell types. For example, recently some MS channels in eukaryotes have been shown to be gated by mechanical force through the lipid membrane similar to bacterial channels (39). In addition, reconstituted bacterial MS channels in mammalian cell membranes were demonstrated to preserve their response to increased membrane tension (40). Synthetic cells reconstituted with MS channels (41, 42) are another potential system where the current model may apply.

Electroporation, sonoporation, and shear stress-induced poration have been used for intracellular delivery of drugs and transfected DNAs. Our work suggests another intracellular delivery method by gating transmembrane MS channels via fluid shear stress. Our results and approach may be useful for designing microfluidic flow channels for shear stress-induced intracellular delivery, which are consistent with recent experimental findings in ref. 25. Although membrane integrity (resealing of the membrane) is an important issue for externally induced membrane poration in other intracellular delivery methods, our proposed method retains the membrane integrity as the tension-driven gating of a MS channel can be achieved before cell lysis under fluid stress (the lysis tension is much larger than the critical tension for opening a MS channel). Also, because bacterial MS channels are typically large enough for the passage of macromolecules, it should be possible to use bacterial MS channels reconstituted into vesicles for drug release (40). However, mammalian MS channels are often smaller, which would limit the size of molecules delivered into mammalian cells.

In our multiscale model the MS channel is assumed to be a cylinder embedded in the lipid membrane. When stretched open by tension in the membrane under fluid stress, the intracellular transport through the MS channel depends on the detailed molecular structures of the channel protein (such as the protein surface charge) and its coupling with the surrounding lipids (9, 13). The present model also does not account for the fluid transport across the membrane when the MS channel is open, which is estimated to be small in cases considered here (see *SI Appendix* for an order of magnitude estimate). Significant change in volume is expected only when multiple MS channels are gated open for extended periods. We are working on incorporating these details into our multiscale continuum model to quantify the mechanosensitivity and efficiency of mechanotransduction of fluid stress by MS channels.

ACKNOWLEDGMENTS. Y.-N.Y., S.V., and H.A.S. acknowledge partial support from National Science Foundation/Division of Mathematical Sciences Grants 1222550, 1224656, and 1219366, respectively.

1. Kung C, Martinac B, Sukharev S (2010) Mechanosensitive channels in microbes. *Annu Rev Microbiol* 64:313–329.
2. Martinac B, Kloda A (2012) Mechanosensory transduction. *Comprehensive Biophysics*, ed Egelman EH (Elsevier, Amsterdam), pp 108–141.
3. Sackin H (1995) Mechanosensitive channels. *Annu Rev Physiol* 57:333–353.
4. Betanzos M, Chiang CS, Guy HR, Sukharev S (2002) A large iris-like expansion of a mechanosensitive channel protein induced by membrane tension. *Nat Struct Biol* 9(9): 704–710.
5. Blount P, Sukharev SI, Schroeder MJ, Nagle SK, Kung C (1996) Single residue substitutions that change the gating properties of a mechanosensitive channel in *Escherichia coli*. *Proc Natl Acad Sci USA* 93(21):11652–11657.
6. Sukharev S, Sachs F (2012) Molecular force transduction by ion channels: Diversity and unifying principles. *J Cell Sci* 125(Pt 13):3075–3083.
7. Sukharev S, Durell SR, Guy HR (2001) Structural models of the MscL gating mechanism. *Biophys J* 81(2):917–936.
8. Kong Y, Shen Y, Warth TE, Ma J (2002) Conformational pathways in the gating of *Escherichia coli* mechanosensitive channel. *Proc Natl Acad Sci USA* 99(9):5999–6004.
9. Ollila OHS, et al. (2009) 3D pressure field in lipid membranes and membrane-protein complexes. *Phys Rev Lett* 102(7):078101.
10. Yoshimura K, Usukura J, Sokabe M (2008) Gating-associated conformational changes in the mechanosensitive channel MscL. *Proc Natl Acad Sci USA* 105(10):4033–4038.
11. Mukherjee N, et al. (2014) The activation mode of the mechanosensitive ion channel, MscL, by lysophosphatidylcholine differs from tension-induced gating. *FASEB J* 28(10): 4292–4302.
12. Phillips R, Ursell T, Wiggins P, Sens P (2009) Emerging roles for lipids in shaping membrane-protein function. *Nature* 459(7245):379–385.
13. Vanegas JM, Arroyo M (2014) Force transduction and lipid binding in MscL: A continuum-molecular approach. *PLoS ONE* 9(12):e113947.
14. Sukharev S, Akitake B, Anishkin A (2007) The bacterial mechanosensitive channel MscS: Emerging principles of gating and modulation. *Curr Top Membr* 58:235–267.
15. Sukharev S, Anishkin A (2004) Mechanosensitive channels: What can we learn from 'simple' model systems? *Trends Neurosci* 27(6):345–351.
16. Belyy V, Anishkin A, Kamaraju K, Liu N, Sukharev S (2010) The tension-transmitting 'clutch' in the mechanosensitive channel MscS. *Nat Struct Mol Biol* 17(4):451–458.
17. Hamill OP, Martinac B (2001) Molecular basis of mechanotransduction in living cells. *Physiol Rev* 81(2):685–740.
18. Martinac B, Buechner M, Delcour AH, Adler J, Kung C (1987) Pressure-sensitive ion channel in *Escherichia coli*. *Proc Natl Acad Sci USA* 84(8):2297–2301.
19. Sachs F (1991) Mechanical transduction by membrane ion channels: A mini review. *Mol Cell Biochem* 104(1–2):57–60.
20. Wiggins P, Phillips R (2004) Analytic models for mechanotransduction: Gating a mechanosensitive channel. *Proc Natl Acad Sci USA* 101(12):4071–4076.
21. Turner MS, Sens P (2004) Gating-by-tilt of mechanically sensitive membrane channels. *Phys Rev Lett* 93(11):118103.
22. Jeon J, Voth GA (2008) Gating of the mechanosensitive channel protein MscL: The interplay of membrane and protein. *Biophys J* 94(9):3497–3511.
23. Bonthuis DJ, Golestanian R (2014) Mechanosensitive channel activation by diffusio-osmotic force. *Phys Rev Lett* 113(14):148101.
24. Sarles SA, Leo DJ (2010) Regulated attachment method for reconstituting lipid bilayers of prescribed size within flexible substrates. *Anal Chem* 82(3):959–966.
25. Najem J, Dunlap M, Sukharev S, Leo DJ (2014) Mechanosensitive channels activity in a droplet interface bilayer system. *MRS Proc* 1621:171–176.
26. Sharei A, et al. (2013) A vector-free microfluidic platform for intracellular delivery. *Proc Natl Acad Sci USA* 110(6):2082–2087.
27. Vlahovska PM, Podgorski T, Misbah C (2009) Vesicles and red blood cells in flow: From individual dynamics to rheology. *C R Phys* 10:775–789.
28. Forsyth AM, Wan J, Owrutsky PD, Abkarian M, Stone HA (2011) Multiscale approach to link red blood cell dynamics, shear viscosity, and ATP release. *Proc Natl Acad Sci USA* 108(27):10986–10991.
29. Haselwandter CA, Phillips R (2013) Directional interactions and cooperativity between mechanosensitive membrane proteins. *Europhys Lett* 101(6):68002p1–68002p6.
30. Wan J, Ristenpart WD, Stone HA (2008) Dynamics of shear-induced ATP release from red blood cells. *Proc Natl Acad Sci USA* 105(43):16432–16437.
31. Bagchi P, Kalluri RM (2009) Dynamics of nonspherical capsules in shear flow. *Phys Rev E Stat Nonlin Soft Matter Phys* 80(1 Pt 2):016307.
32. Veerapaneni SK, Gueyffier D, Zorin D, Biros G (2009) A boundary integral method for simulating the dynamics of inextensible vesicles suspended in a viscous fluid in 2D. *J Comput Phys* 2009:2334–2353.
33. Veerapaneni SK, Rahimian A, Biros G, Zorin D (2011) A fast algorithm for simulating vesicle flows in three dimensions. *J Comput Phys* 230:5610–5634.
34. Haselwandter CA, Phillips R (2013) Connection between oligomeric state and gating characteristics of mechanosensitive ion channels. *PLoS Comput Biol* 9(5):e1003055.
35. Huang HW (1986) Deformation free energy of bilayer membrane and its effect on gramicidin channel lifetime. *Biophys J* 50(6):1061–1070.
36. Pozrikidis C (1987) Creeping flow in two-dimensional channels. *J Fluid Mech* 180:495–514.
37. Phillips R, Kondev J, Theriot J, Garcia HG (2012) *Physical Biology of the Cell* (Garland Science, Taylor and Francis Group, New York).
38. Yoshimoto M, Tamura R, Natsume T (2013) Liposome clusters with shear stress-induced membrane permeability. *Chem Phys Lipids* 174:8–16.
39. Brohawn SG, Su Z, MacKinnon R (2014) Mechanosensitivity is mediated directly by the lipid membrane in TRAAK and TREK1 K^+ channels. *Proc Natl Acad Sci USA* 111(9): 3614–3619.
40. Doerner JF, Febvay S, Clapham DE (2012) Controlled delivery of bioactive molecules into live cells using the bacterial mechanosensitive channel MscL. *Nat Commun* 3:990.
41. Heureaux J, Chen D, Murray VL, Deng CX, Liu AP (2014) Activation of a bacterial mechanosensitive channel in mammalian cells by cytoskeletal stress. *Cell Mol Bioeng* 7(3):307–319.
42. Lee LM, Liu AP (2015) A microfluidic pipette array for mechanophenotyping of cancer cells and mechanical gating of mechanosensitive channels. *Lab Chip* 15(1):264–273.